Xu, Gang; Zhu, Guoqing; Pan, Rongliang; Liu, Xin

Investigation on temperature distribution under the coupling action of transverse position and fire sealing of linear fire in tunnel

Published in:
Case Studies in Thermal Engineering

DOI:
10.1016/j.csite.2021.101032

Published: 01/08/2021

Document Version
Publisher's PDF, also known as Version of record

Please cite the original version:
Xu, G., Zhu, G., Pan, R., & Liu, X. (2021). Investigation on temperature distribution under the coupling action of transverse position and fire sealing of linear fire in tunnel. *Case Studies in Thermal Engineering*, *26*, Article 101032. https://doi.org/10.1016/j.csite.2021.101032

Case Studies in Thermal Engineering 26 (2021) 101032

Contents lists available at ScienceDirect

Case Studies in Thermal Engineering

journal homepage: www.elsevier.com/locate/csite

Investigation on temperature distribution under the coupling action of transverse position and fire sealing of linear fire in tunnel

Gang Xu [a,b], Guoqing Zhu [a,b,*], Rongliang Pan [a,b,c], Xin Liu [a,b]

[a] Jiangsu Key Laboratory of Fire Safety in Urban Underground Space, China University of Mining and Technology, Xuzhou, 221116, China
[b] Institute of Public Safety and Fire Engineering, China University of Mining and Technology, Xuzhou, 221116, China
[c] Department of Civil Engineering, Aalto University, FI-00076, AALTO, Finland

ARTICLE INFO

Keywords:
Fire characteristics
Fireproof sealing
Linear fire source
Longitudinal temperature distribution
Maximum ceiling temperature rise

ABSTRACT

By sealing the portal at one end of tunnel and changing the transverse location of linear fire source in tunnel, the hot smoke layer, longitudinal temperature distribution and maximum temperature of linear fire source were investigated. It is found that the flame will bend under the influence of curved ceiling and hot smoke layer will be thicker when the linear fire source approaches to the side wall. The variation law of heat release rate is analyzed by considering the limiting effect of side wall and thermal feedback. By modifying the previous formula of effective ceiling height, an empirical formula for predicting longitudinal temperature distribution of linear fire sources with different aspect ratios is proposed, and the ventilation coefficient is obtained to characterized the temperature under sealing and without sealing. Moreover, the accuracy of predicted temperature under sealing is verified by using the ventilation coefficient. Based on dimensional analysis, it's concluded that the maximum temperature mainly depends on the heat release rate, and an empirical formula is proposed to predict the maximum temperature rise of linear fire sources with different aspect ratios in several transverse positions. The error of predicted values and actual values is within 13%.

1. Introduction

The utility tunnel is an important public facility and many cables are placed in there. Thus, fire occurred in tunnel will cause serious damage. The burning cable can be regarded as a linear fire source, and the cable layout can be simulated by changing the transverse position of linear fire source in fire research. Investigation of linear fire characteristics is helpful for the fire protection work in utility tunnel.

The tunnel fire has been researched by many scholars [1–8]. A series of experiments have conducted to investigate flame height and fire characteristics of linear fire with different aspect ratios. Ji et al. [9] studied the combustion characteristics of n-heptane fires with different aspect ratios, and found that the aspect ratio has little effect on the flame morphology and radiation distribution of linear pool fires when the width of the oil pool is constant. Chuan Gang Fan [10] investigated the influence of sidewall, it was found that more extended flame heating sidewall and the heat feedback from sidewall increased when the aspect ratio of fire increased, which also caused the mass loss rate rose. However, the flame height of n-heptane decreased because the oxygen needed for complete combustion of n-heptane was 1.56 times than that of ethanol, while the flame height of methanol fire increased. Zhou et al. [11] found the aspect

* Corresponding author. School of Safety Engineering, China University of Mining and Technology, Xuzhou 221116, China.
E-mail address: zgq119xz@cumt.edu.cn (G. Zhu).

https://doi.org/10.1016/j.csite.2021.101032
Received 10 February 2021; Received in revised form 14 April 2021; Accepted 21 April 2021
Available online 5 May 2021

List of symbols

$\dot{Q}$	Heat release rate of linear fire source(kW)
$\dot{Q}^*$	Dimensionless heat release rate of linear fire source
ΔH	Complete combustion heat of fuel(kJ/g)
$T_{s,x}$	Ceiling temperature at location x from the center of the fire source under sealing(K)
$T_{s,\max}$	Maximum ceiling temperature at location x from the center of the fire source under sealing (K)
$T_{o,x}$	Ceiling temperature at location x from the center of the fire source without sealing(K)
$T_{o,\max}$	Maximum ceiling temperature at location x from the center of the fire source without sealing (K)
T_0	Ambient temperature(°C)
ΔT_x	Ceiling temperature rise from the center of the fire source(K)
$\Delta T_{\max}$	Maximum ceiling temperature rise (K)
ΔT^*_{max}	Dimensionless maximum ceiling temperature rise
$\Delta T^*_{s,max}$	Dimensionless maximum ceiling temperature rise under sealing
$\Delta T^*_{o,max}$	Dimensionless maximum ceiling temperature rise without sealing
$\dot{m}''_0$	Mass loss rate per unit area(kg/(sm^2))
$\dot{m}''_\infty$	Asymptotic value for mass loss rate per unit area(kg/(s·m^2))
$\dot{m}$	Mass loss rate of linear fire source(g/s)
x	Longitudinal distance from the center of the linear fire source(m)
$Y_{ox,l}$	Oxygen fraction feeding the flame
$Y_{ox,o}$	Oxygen fraction in the free burning
$\dot{q}_{External}$	Heat feedback from external environment(kW/m^2)
L	Heat of gasification(kJ/kg)
$A_{F,b}$	Fuel burning area(m^2)
H	Vertical height from the bottom of fire source to the ceiling(m)
H_{ef}	Effective ceiling height(m)
H'_{ef}	Modified effective ceiling height(m)
R	Radius of the tunnel(m)
r	Arc length from the plume impact point to the ceiling center (m)
θ	The angle between the impinge point and the tunnel centerline(°)
l	Transverse distance from the centerline of the tunnel(cm)
d	Length of the linear fire source(m)
c_p	The specific heat capacity of ambient air at constant pressure(J/(kg ·K))
g	Acceleration of gravity(m/s^2)
ρ_0	Density of ambient air(kg/m^3)
χ	Average combustion efficiency
D	Pool equivalent diameter(m)
γ	Ventilation coefficient

ratio of fire source has limited influence on the maximum temperature rise, while the effective ceiling height has great influence on the maximum temperature by changing central angle between linear source and ceiling center. A modified first order non-homogeneous linear differential equation was proposed based on the model of Ingason, which can predict the longitudinal temperature distribution of linear fire source with different aspect ratio.

In reality, location of fire is relatively random due to the multi-layer arrangement of combustibles in the utility tunnel, which causes fire extinguishing system occupied in tunnel can't put out the fire accurately, so the fire sealing is usually used to control fire in tunnel.

Many scholars have conducted a series of experiments to study combustion parameters of fire when sealing the tunnel portal. Yao et al. [12] conducted the experiment in a reduced-scale closed rectangular tunnel. It was found that the flame would bend to the nearest closed end when the fire source deviated from tunnel center, the maximum temperature would decrease with the increase of flame angle. A modified formula to predict the maximum temperature in enclosed tunnel under a series of boundary conditions was proposed. Chen et al. [13] investigated the maximum ceiling temperature of tunnel fire theoretically, experimentally and numerically, and concluded that sealing ratio had great influence on maximum ceiling temperature. Moreover, a critical sealing ratio was obtained, the maximum gas temperature will decrease gradually when beyond the critical sealing ratio. Besides, an empirical model to predict

(a) The reduced-scale tunnel

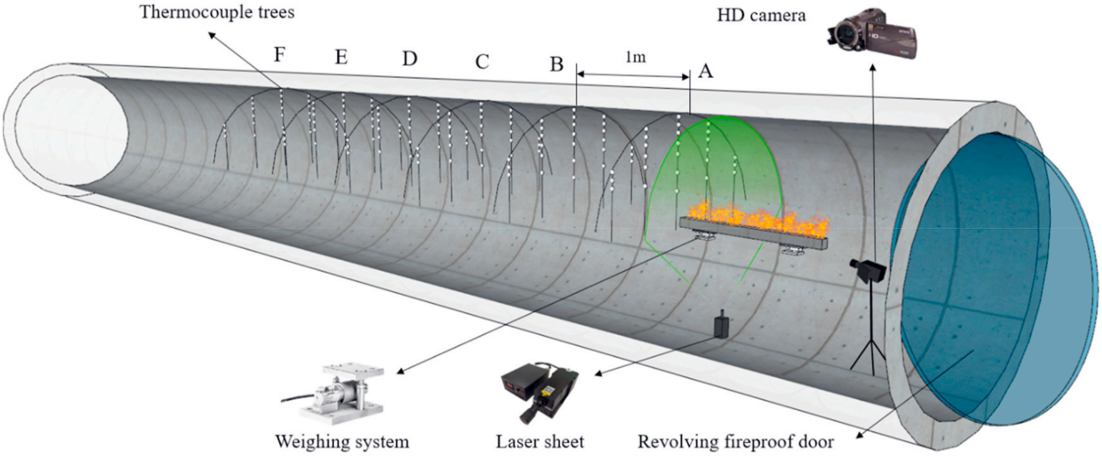

(b) Arrangement of experimental devices in reduce-scale tunnel

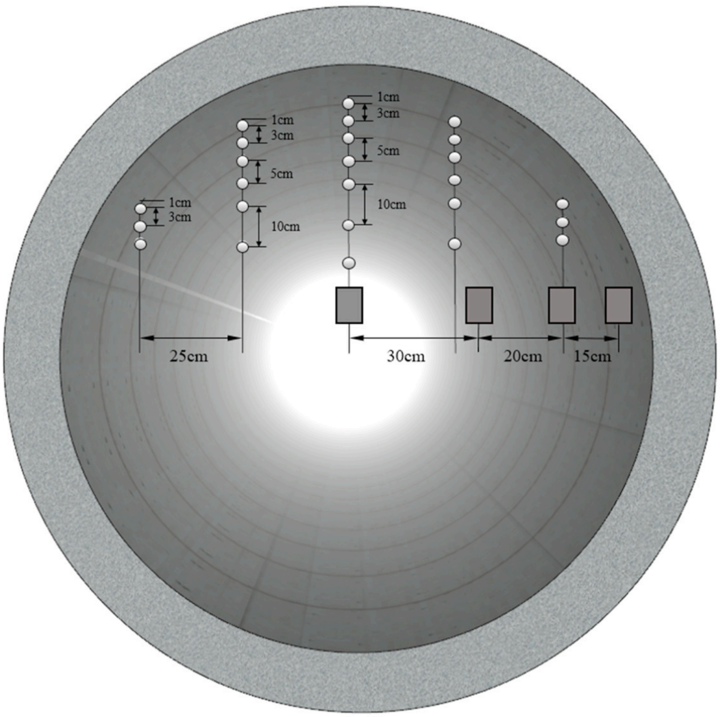

(c) Location of fire source and arrangement of thermocouples in cross section

(caption on next page)

Fig. 1. Diagram of experimental setup.
(a) The reduced-scale tunnel
(b) Arrangement of experimental devices in reduce-scale tunnel
(c) Location of fire source and arrangement of thermocouples in cross section

the maximum ceiling temperature is developed. Liu et al. [14] carried out experiments in a reduced-scale circular tunnel, and found that the gas temperature appeared obvious stratification in the vertical direction. Considering the effect of ceiling jet temperature, the prediction formula of maximum ceiling temperature proposed by Li [15] was modified that derived from the energy conservation equation.

Lots of experiments conducted by predecessors were in the rectangular tunnel, while the investigations in curved ceiling tunnel are less. The circular tunnel has a curved ceiling compared with the rectangular tunnel, which reduces the heat exchange with the external environment and thickness of hot smoke layer is larger. Moreover, accumulation of heat in the center of curved ceiling will cause thermal damage to concrete structure. In addition, the thermal feedback will affect the combustion of fire source. Thus, experiments are carried out in a reduced-scale tunnel, and linear fire source with three aspect ratios is put on different transverse location when portal is under sealing and without sealing. The hot smoke layer, longitudinal temperature distribution and the maximum temperature rise are investigated. Moreover, a modified empirical equation to predict the longitudinal ceiling temperature distribution is proposed. Based on dimensional analysis, an empirical formula for predicting the maximum ceiling temperature rise is also proposed. Also, it's found that the ventilation coefficient can characterize the relationship of the temperature under different sealing condition. Investigation provides some reference significance for the structural fire resistance design and fire control work in underground utility tunnel.

2. Experiment

According to the Froude similarity criterion, the experiment was conducted in a reduced-scale circular tunnel with length 20 m and radius 0.75 m. A revolving fire proof door was installed at one end of tunnel as sealed portal. The tunnel model is shown in Fig. 1 (a).

$$\begin{aligned} \dot{Q}_{c,M} &= \dot{Q}_{c,F}\left(\frac{l_M}{l_F}\right)^{5/2} \\ M_{c,M} &= M_{c,F}\left(\frac{l_M}{l_F}\right)^{5/2} \\ t_{c,M} &= t_{c,F}\left(\frac{l_M}{l_F}\right)^{5/2} \\ T_{c,M} &= T_{c,F} \end{aligned} \tag{1}$$

Eq. (1) is the Froude similarity criterion formula, where M represents reduced-scale model experiment while F represents full-scale experiment.

Linear fire sources are with three lengths of 1.9 m, 1.7 m and 1.5 m, 4 cm in width and 5 cm in height, and the aspect ratios are 47.5, 42.5 and 37.5, respectively. When the aspect ratio is greater than 10, the fire source can be regarded as a linear fire source [16], use n-heptane as fuel. Besides, the fire source is at the height of 20 cm vertically from the center of the tunnel, and at the transverse positions of 0 cm, 30 cm, 50 cm, and 65 cm, respectively. The fire source position is shown in Fig. 1(c), and the ambient temperature is 27 °C.

Laser sheet below the fire source can illuminate the smoke particles. And a HD camera records the flame shape and smoke flow.

The weighing equipment used in experiment is SIWAREX weighing sensors with range of 0–10 kg, which has sampling frequency for 1 s/time so that the process of quality changing of fire source can be recorded accurately. Thus, the mass loss rate is obtained and the heat release can be calculated by using Eq. (2). ΔH is the combustion heat of n-heptane, 44.4 kJ/g χ is the average combustion coefficient, which is 0.92 when the portal is sealed, while coefficient is 0.75 when the portal is without sealing. $\dot{m}$ is the mass loss rate, g/s [17,18].

$$\dot{Q} = \chi \cdot \dot{m} \cdot \Delta H \tag{2}$$

The hot gas of fire rises vertically and spreads horizontally after hitting the ceiling, so the maximum temperature exists in the position closest to the ceiling. In order to measure the smoke temperature near the ceiling more accurately, the distance of thermocouples and ceiling is 1 cm to avoid direct contact [11]. The temperature distribution of ceiling jet in the vertical direction showed top-hat distribution with a bulging shape. Besides, the thickness of temperature layer with rapid temperature rise is tiny, and with large

Table 1
Summary of experimental tests.

Number	Length	l	Portal	Quality	Number	Length	l	Portal	Quality
1	1.5 m	0 cm	Open	307g	13	1.5 m	0 cm	Sealed	306g
2	1.5 m	30 cm	Open	304g	14	1.5 m	30 cm	Sealed	307g
3	1.5 m	50 cm	Open	306g	15	1.5 m	50 cm	Sealed	304g
4	1.5 m	65 cm	Open	305g	16	1.5 m	65 cm	Sealed	306g
5	1.7 m	0 cm	Open	308g	17	1.7 m	0 cm	Sealed	305g
6	1.7 m	30 cm	Open	306g	18	1.7 m	30 cm	Sealed	305g
7	1.7 m	50 cm	Open	304g	19	1.7 m	50 cm	Sealed	304g
8	1.7 m	65 cm	Open	305g	20	1.7 m	65 cm	Sealed	306g
9	1.9 m	0 cm	Open	306g	21	1.9 m	0 cm	Sealed	307g
10	1.9 m	30 cm	Open	305g	22	1.9 m	30 cm	Sealed	305g
11	1.9 m	50 cm	Open	304g	23	1.9 m	50 cm	Sealed	307g
12	1.9 m	65 cm	Open	306g	24	1.9 m	65 cm	Sealed	306g

temperature gradient in this layer. Therefore, the spacing of the thermocouple is set closely in this layer [19]. Arrangement of experimental devices and thermocouples is as shown in Fig. 1(b) and (c). All experimental tests are listed in Table 1.

3. Results and discussion

3.1. Hot smoke layer

The hot smoke will spread along the ceiling when fire occurs, which will accumulate under the tunnel ceiling and cause damage to concrete structure. Thus, investigation of transverse temperature distribution and smoke flow of the hot smoke has reference significance for the protection design of structure and the installation of fire detectors in tunnel. Cables are usually laid close to the side walls in utility tunnel. Therefore, working conditions at L = 50 cm and L = 65 cm were selected to analyze the hot somke layer in the stable combustion stage, as shown in Fig. 2(a) and Fig. 2(b).

Fig. 2(a) and (b) show that plume impact zone is located vertically above the fire source. Also, the hot smoke hit the ceiling vertically at first when the fire source near the wall, then flows along the curved ceiling. When the hot smoke flows to the side that away from fire source, it no longer spreads vertically downward but horizontally spreads towards to the fire source, and the smoke entrains air and forms a number of vortices. By comparing Fig. 2(a) and (b), when fire source approaches to side wall, the flame will be bent under the influence of curved ceiling, which resulting a thicker hot smoke layer.

Fig. 2(c) is transverse temperature distribution under curved ceiling. The temperature directly above the fire source is the highest and decreases along the direction away from the fire source, which is consistent with the flow law of the hot smoke layer in Fig. 2 (a) and Fig. 2 (b).

3.2. Heat release rate

Circular tunnel has arc-shaped structure, so curved ceiling will accumulate more hot smoke under ceiling center than flat ceiling, which will cause damage to the structure. When linear fire approaches to the side wall, air entrained of plume is not symmetrical due to the ceiling constraint effect, then affects heat release rate. Sealing portal will also affect the air entrainment of fire plume in the longitudinal direction. Fig. 3 shows the varying tendencies of heat release rate in the process of fire sources moving towards the side wall under sealing and without sealing.

According to Eq. (2), when the fuel type and combustion efficiency are determined, the heat release rate is related to the mass loss rate. Investigating the parameters that affect the mass loss rate is helpful to study the change of heat release rate. Previous researchers have conducted fairly extensive pool-fire experiments with a variety of liquids. It is found that when the diameter is greater than 0.2 m, the combustion rate increases with the increase of pool diameter, and when it reaches a certain value, it is called the asymptotic diameter mass loss rate, which is generally expressed as $\dot{m}''_{\infty}$, kg/(m^2·s).The mass loss rate of a pool fire is affected by the pool diameter and two empirical constants that depend on the type of fuel used, the two constants are extinction -absorption of the flame, k, and mean beam length corrector, β. A lot of free combustion experiments were conducted for liquids with different diameters, and Eq. (3) [20, 21],was obtained.

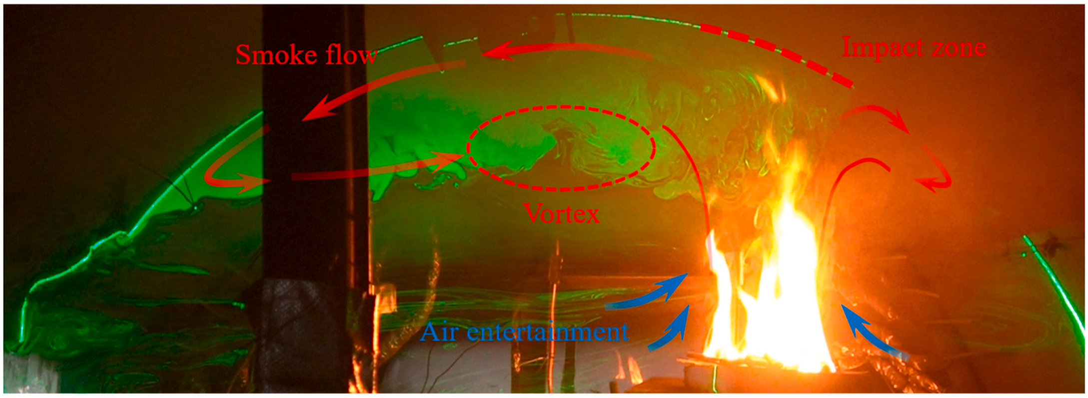

(a) The fire source is in 50 cm from the center and without sealing

(b) The fire source is in 65 cm from the center and without sealing

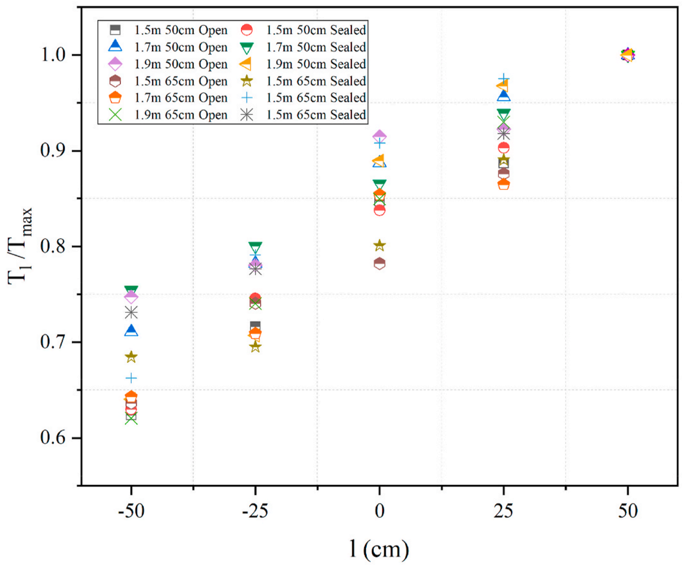

(c) Transverse temperature distribution under curved ceiling

(caption on next page)

Fig. 2. The hot smoke layer and transverse temperature distribution.
(a) The fire source is in 50 cm from the center and without sealing
(b) The fire source is in 65 cm from the center and without sealing
(c) Transverse temperature distribution under curved ceiling

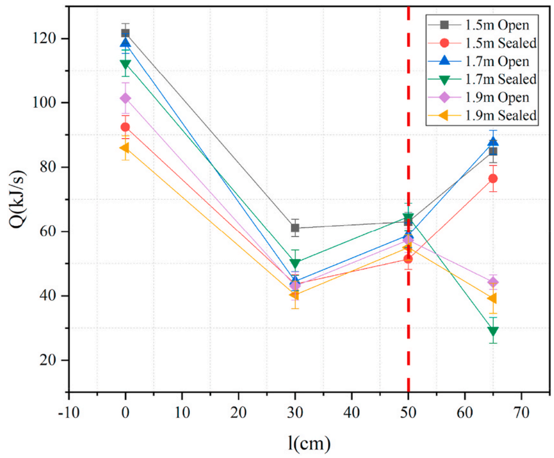

Fig. 3. The heat release rate of all experimental tests.

$$\dot{m}_0'' = \dot{m}_\infty'' \cdot \left(1 - e^{-k\beta D}\right) \tag{3}$$

$\dot{m}_0''$ is the free burn mass loss rate per unit area. $\dot{m}_\infty''$ and $k\beta$ depending on the liquid type. $\dot{m}_\infty''$ is 0.075 kg/(m^2·s) for n-heptane [21], and D is equivalent diameter for linear pool fire, m. The mass loss rate can be expressed as follows:

$$\dot{m} = \dot{m}_0'' A_{F,b} \frac{Y_{ox,l}}{Y_{ox,o}} + \frac{\dot{q}_{External}}{L} \tag{4}$$

Where $A_{F,b}$ is the surface area of the combustion fuel. $Y_{ox,l}$ is the oxygen fraction of the feed flame. $Y_{ox,o}$ is the oxygen fraction of the free combustion fire source. $\dot{q}_{External}$ is the feedback heat flow of the external environment. And L is the heat of vaporization. Substituting Eq. (3) into Eq. (4), we can get:

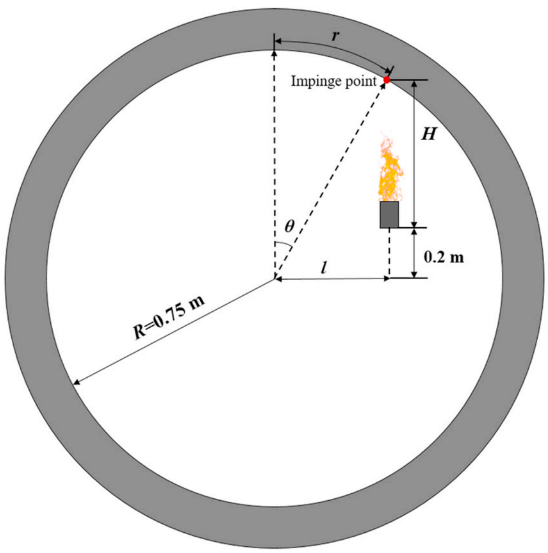

Fig. 4. The schematic of modified effective ceiling height.

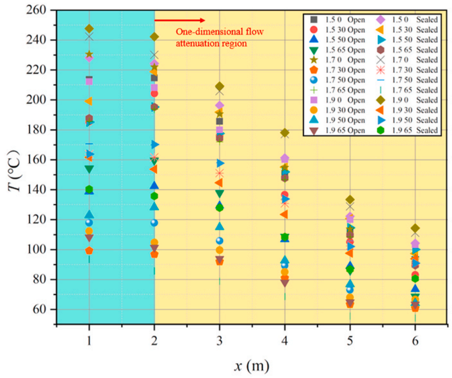

(a) The longitudinal temperature distribution of all experimental tests

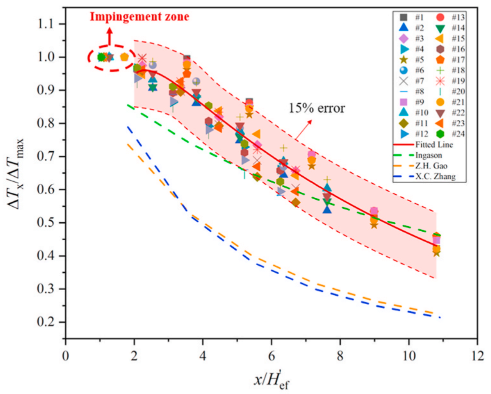

(b) Correlation of dimensionless temperature rise and the dimensionless length

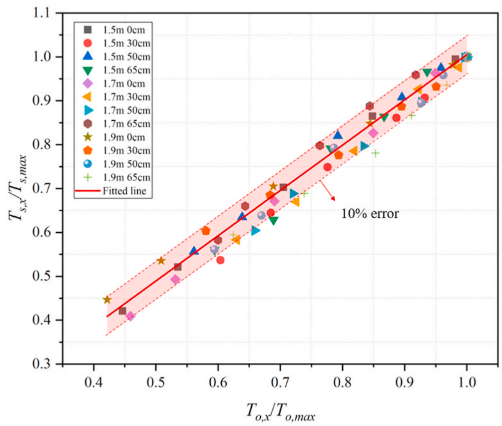

(c) Correlation of $T_{s,x}$ / $T_{s,\max}$ and $T_{o,x}$ / $T_{o,\max}$

Fig. 5. Correlation of longitudinal temperature when portal is in different sealing situation.
(a) The longitudinal temperature distribution of all experimental tests
(b) Correlation of dimensionless temperature rise and the dimensionless length
(c) Correlation of $T_{s,x}$ / $T_{s,\max}$ and $T_{o,x}$ / $T_{o,\max}$

$$\dot{m}=\dot{m}_{\infty}''\cdot\left(1-e^{-k\beta D}\right)A_{F,b}\frac{Y_{ox,l}}{Y_{ox,o}}+\frac{\dot{q}_{External}}{L} \tag{5}$$

The variety of heat release rate in Fig. 3 can be analyzed by Eq. (5). On the left side of red dotted line, the heat release rates of the three sizes of fire sources have the same changing trend of decreasing first and then increasing, which as shown in Fig. 3. In the process of moving from the center to the sidewall, the thermal feedback received from the sidewall strengthens $\dot{q}_{External}$ in Eq. (5). Thus, the heat release rate increases under the effect of thermal feedback. On the right side of red dotted line, fire directly heated the wall and thermal feedback received from the wall increased, then the heat release rate of fire source with 1.5 m length continued to increase. Heat release rate of fire source with 1.7 m length is reduced, that with 1.9 m length decreased. When burning surface area ($A_{F,b}$) is larger, the demand for oxygen sis greater. When fire source against wall, only the non-wall-side entrains air, as Fig. 2 (a) and Fig. 2 (b). Sealing portal can also affect the air flow and oxygen supply in the tunnel, resulting in a loss of $Y_{ox,l}$ in Eq. (5) and the mass loss rate decreases [22,23].

With the insufficient oxygen supply and the restriction of side wall, sealing portal has a certain influence on combustion of fire source with aspect ratio greater than 42.5:1 near the side wall. The reasons are the side wall constraint effect and lack of oxygen supply. More oxygen is needed for combustion when the fire area is larger, so fire source combustion will be restricted by insufficient oxygen supply.

3.3. Longitudinal temperature distribution

When fire occurs in tunnel, hot plume first rises vertically and hits the ceiling, and ceiling jet then moves toward the opposite direction along curved ceiling. When fire reaches stable stage, the ceiling jet develops from a radial flow to a one-dimensional flow along the longitudinal direction of tunnel. It is instructive to investigate the longitudinal temperature distribution of ceiling jet for the placement of fire detectors in the tunnel. The longitudinal temperature distribution of all working conditions as shown in Fig. 5(a). The temperature tends to be consistent in the range of $x<2$ m. When $x>2$ m, the ceiling jet forms a stable one-dimensional flow and temperature attenuation accelerates along the longitudinal direction. The longitudinal temperature distribution of fire source is affected by effective ceiling height. Ingason et al. [24] proposed a formula to predict the longitudinal temperature distribution under ceiling:

$$\frac{\Delta T_x}{\Delta T_{\max}}=A_1\cdot\exp\left(-a_1\frac{x}{H_{ef}}\right)+A_2\cdot\exp\left(-a_2\frac{x}{H_{ef}}\right) \tag{6}$$

When studying the fire in rectangular tunnel, H_{ef} is usually expressed by the vertical distance between fire source and flat ceiling. While the circular tunnel has a curved ceiling, which causes a thicker smoke layer than rectangular tunnel. Therefore, it is necessary to make corrections about H_{ef} in the circular tunnel. When the fire occurs, plume will spread along curved ceiling after impinged on the ceiling vertically. The vertical distance between fire source and plume impinge point and the arc length from impinge point to ceiling center is taken as the modified effective ceiling height $H_{ef}^{'}$, as shown in Fig. 4, which can be expressed as:

$$H_{ef}^{'}=H+r \tag{7}$$

$$H=\sqrt{R^2-l^2}-0.2 \tag{8}$$

$$\theta=\arcsin\frac{l}{R} \tag{9}$$

$$r=\frac{\theta\pi R}{180} \tag{10}$$

H represents the vertical height from fire source bottom to the impinge point, m. r represents the arc length between impinge point and ceiling center, m.

The modified equation can be obtained from Fig. 4, the modified effective ceiling height are listed in Table 2:

$$H_{ef}^{'}=\sqrt{R^2-l^2}-0.2+\frac{\pi R}{180}\arcsin\frac{l}{R} \tag{11}$$

Table 2
The modified effective ceiling height in different transverse locations.

l (cm)	0	30	50	65
$H_{ef}^{'}$ (m)	0.55	0.7974	0.9090	0.9651

Substituting the revised equation into Eq. (6), the relationship of dimensionless temperature rise $\Delta T_x/\Delta T_{\max}$ and dimensionless length x/H'_{ef} can be obtained, as shown in Fig. 5(b).

Thus, Eq. (12) is proposed to predict longitudinal temperature distribution of linear fire with different aspect ratios under sealing and without sealing.

$$\frac{\Delta T_x}{\Delta T_{\max}} = -3.443 \cdot \exp\left(-1.754\frac{x}{H'_{ef}}\right) + 1.289 \cdot \exp\left(-0.104\frac{x}{H'_{ef}}\right) \tag{12}$$

The dimensionless temperature rise and dimensionless length show good correlation obtained by Eq. (12) is as shown in Fig. 5(b), and the predicted temperature is higher than the previous results [24–26]. That's because the formula of Ingason, Z.H. Gao and X.C. Zhang is proposed from the experiment with flat ceiling, and thicker smoke layer causes higher ceiling temperature due to the smoke accumulation under curved ceiling. It should be noted that modified Eq. (12) only applies of the $x > d/2$ area, and impact zone of fire plume is in the $x \leq d/2$ area, where $\Delta T_x/\Delta T_{\max}$ is always 1.

When portal is sealed, oxygen supply near the fire source is insufficient, which will affect mass loss rate and longitudinal temperature distribution. The temperature of the fire source with same aspect ratio at same position shows a correlation under different sealing conditions. The correlation can be expressed by Eq. (13).

$$\frac{T_{s,x}}{T_{s,\max}} \propto \frac{T_{o,x}}{T_{o,\max}} \tag{13}$$

$T_{o,x}$ And $T_{s,x}$ is temperature under ceiling at longitudinal location x from fire source when portal is under sealing and without sealing, $T_{o,\max}$ and $T_{s,\max}$ is the longitudinal maximum temperature under ceiling when portal is under sealing and without sealing. Since the heat release rate is affected by ventilation condition, ventilation coefficient γ is proposed to characterize the relationship between the temperature ratio under different sealing situation.

$$\frac{T_{s,x}}{T_{s,\max}} = f(\gamma)\frac{T_{o,x}}{T_{o,\max}} \tag{14}$$

The relationship in Eq. (14) is shown in Fig. 5(c). $T_{s,x}/T_{s,\max}$ and $T_{o,x}/T_{o,\max}$ show a linear correlation and the correlation coefficient is 0.99. The ventilation coefficient γ is obtained as 1.12, which is a constant. The ventilation coefficient can be used to predict longitudinal temperature distribution when portal is sealed.

3.4. Maximum temperature rise under ceiling

According to previous research, a fire partition in utility tunnel is generally 200 m. When fire occurs in a fire partition, fire door of adjacent fire partition will be closed, and it will be opened again after the fire is extinguished. In some fire scenarios, maximum temperature in a portal-sealed tunnel will be higher than that in the actual tunnel fire. The fire sealing will limit the oxygen supply and affect the heat release rate of fire source. In order to characterize the influence of fireproof sealing on fire, Fig. 6(a) shows the temperature curve of working conditions #3 and #15.

It can be seen from Fig. 6(a) that sealing portal will increase the maximum temperature and accelerate the decay rate of heat due to insufficient oxygen supply. The main reasons are fireproof sealing reduce smoke emission and heat loss, and much thermal feedback from surroundings will increase the heat release rate [13].Which will affect the maximum temperature. Thus, it's necessary to analyze the dominant factor that affect heat release rate. Fig. 6(b) shows the relationship of $\Delta T_{\max}/T_0$ and dimensionless heat release rate $\dot{Q}^*$, it's found that $\dot{Q}^*$ increases with the increase of $\Delta T_{\max}/T_0$, so it can be concluded that maximum temperature under ceiling is mainly influenced by heat release rate.

Excessive maximum temperature will damage the tunnel structure, so it is an important parameter in tunnel fire research. Predecessors conducted a series of experiments to study the maximum ceiling temperature rise. Li et al. [15,27],conducted experiments in a reduced-scale tunnel and proposed an empirical formula for predicting the maximum temperature rise under different wind speeds:

$$\Delta T_{\max} = \begin{cases} \dfrac{\dot{Q}}{Vb^{1/3}H_{ef}{}^{5/3}}, & V' > 0.19 \\[2ex] 17.5\left(\dfrac{\dot{Q}}{H_{ef}^{5/3}}\right)^{2/3}, & V' \leq 0.19 \end{cases} \tag{15}$$

Therein

$$V' = \frac{V}{\left(\frac{g\dot{Q}^{2/3}}{b\rho_a c_p T_a}\right)^{1/3}} \tag{16}$$

It can be seen that $\Delta T_{\max}$ is related to heat release rate $\dot{Q}$ and effective ceiling height H_{ef}.

Kurioka et al. [28] proposed a formula to predict the maximum temperature rise:

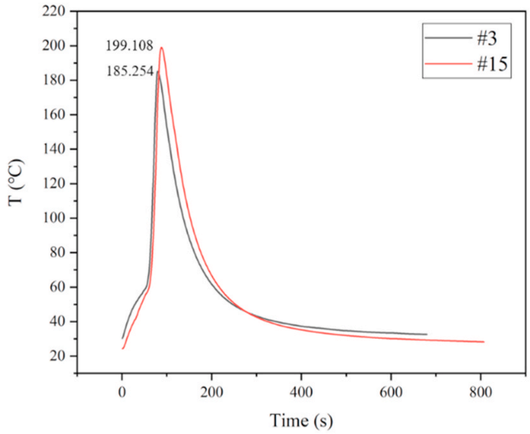

(a) Temperature changing curve of #3 and #15

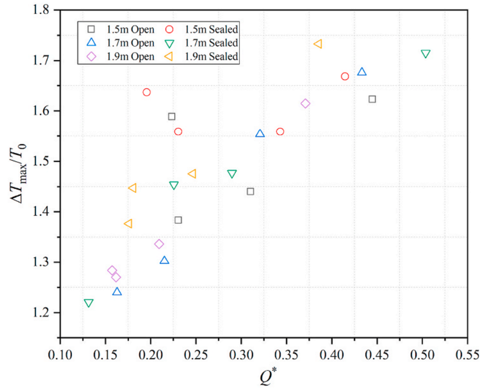

(b) Correlation graph of dimensionless heat release rate and $\Delta T_{\max}/ T_0$

Fig. 6. Comparison of temperature and the effect of heat release rate.
(a) Temperature changing curve of #3 and #15
(b) Correlation graph of dimensionless heat release rate and $\Delta T_{\max}/ T_0$

$$\frac{\Delta T_{\max}}{T_0} = \gamma \left(\frac{\dot{Q}^{*2/3}}{Fr^{1/3}} \right)^{\varepsilon} \tag{17}$$

Wherein , $\begin{matrix} \gamma = 1.77 \quad \varepsilon = 1.2 \ (\dot{Q}^{*2/3}/Fr^{1/3}) < 1.35 \\ \gamma = 2.54 \quad \varepsilon = 0 \quad (\dot{Q}^{*2/3}/Fr^{1/3}) \geq 1.35 \end{matrix}$

$$\dot{Q}^{*} = \frac{\dot{Q}}{\rho_\infty c_p T_\infty g^{1/2} H_{ef}^{5/2}} \tag{18}$$

$$Fr = \frac{V^2}{gH_{ef}} \tag{19}$$

Fr is 0 when the wind speed V is equal to 0. Eq. (17) does not apply to low wind speed conditions.

Previous studies by scholars have found that the maximum temperature rise are related to air temperature, density of air, specific heat capacity of air, gravitational acceleration, heat release rate, and the location of fire source in tunnel [12,29]. The effective ceiling height will change when the fire approaches to the sidewall, so the effective ceiling height can represent the position of fire source. The relationship of maximum ceiling temperature rise and the related parameters above can be expressed as Eq. (20).

$$\Delta T_{\max} = f\left(\dot{Q}, H_{ef}, T_0, \rho_0, c_p, g\right) \tag{20}$$

T_0、ρ_0、c_p and g in Eq. (20) are all constants, so Eq. (20) can be expressed as Eq. (21)

Table 3
Comparison of predicted values and experimental values of dimensionless maximum temperature rise.

Condition	$\Delta T^*_{s,max}$	$\gamma\Delta T^*_{o,max}$	Condition	$\Delta T^*_{s,max}$	$\gamma\Delta T^*_{o,max}$
1.5 m 0 cm	4.023	4.087	1.7 m 50 cm	44.215	45.189
1.5 m 30 cm	34.075	32.436	1.7 m 65 cm	65.724	67.215
1.5 m 50 cm	53.800	53.466	1.9 m 0 cm	4.493	4.721
1.5 m 65 cm	58.786	60.357	1.9 m 30 cm	32.618	34.218
1.7 m 0 cm	3.405	4.203	1.9 m 50 cm	47.593	48.658
1.7 m 30 cm	26.265	25.735	1.9 m 65 cm	63.255	64.746

$$\frac{\Delta T_{\max}}{T_0} = f\left(\frac{\dot{Q}}{\rho_0 c_p T_0 g^{1/2} H_{ef}^{5/2}}, H_{ef}\right) \tag{21}$$

Wherein, $\dot{Q}^* = \frac{\dot{Q}}{\rho_0 c_p T_0 g^{1/2} H_{ef}^{5/2}}$ in Eq. (21), and Eq. (21) can be modified as:

$$\frac{\Delta T_{\max}}{T_0} = f\left(\dot{Q}^*, H_{ef}\right) \tag{22}$$

$$\frac{\Delta T_{\max}}{T_0 \dot{Q}^*} = \phi\left(H_{ef}\right) \tag{23}$$

$\frac{\Delta T_{\max}}{T_0 \dot{Q}^*}$can be expressed by $\Delta T^*_{\max}$in Eq. (23), so Eq. (23) can be simplified as:

$$\Delta T^*_{\max} = \phi\left(H_{ef}\right) \tag{24}$$

The ventilation coefficient has been proposed in section 3.3, the experiment value $\Delta T^*_{s,max}$ and the predicted values $\gamma\Delta T^*_{o,max}$ are listed in Table 3. It can be obtained that the experimental dimensionless maximum temperature rise and the predicted values are nearly. Thus, the ventilation coefficient γ can be used to predict the temperature under sealing.

H_{ef} in Eq. (24) can be modified by H'_{ef} in Eq. (11), the correlation of H'_{ef} and ΔT^*_{max} is shown in Fig. 7(a).

It can be seen from Fig. 7(a) that the dimensionless maximum temperature rise ΔT^*_{max} increases with the increase of H'_{ef}.Therefore, the formula of dimensionless maximum temperature rise and modified effective ceiling height is shown in Eq. (25).

$$\Delta T^*_{\max} = 5.693 \exp \cdot \left(2.793 H'_{ef}\right) - 22.368 \tag{25}$$

The R^2 of the fitting curve reached 0.9878, which indicates a high degree of fitting. Fig. 7 (b) shows the relationship of dimensionless maximum temperature rise predicted by Eq. (25) and the maximum temperature rise obtained from the experiment. The error of predicted value and experimental value is less than 13%. Therefore, the maximum temperature rise of linear fire source at different transverse positions in tunnel can be predicted with Eq. (25) under different sealing conditions.

4. Conclusions

A series of experiments were conducted in a reduced-scale tunnel. And the combustion of linear fire source with three aspect ratios in different transverse positions was studied. The longitudinal temperature distribution, maximum ceiling temperature rise and temperature of smoke layer are investigated under the coupling effect of sealing portal and different transverse position of linear fire source. The main conclusions are：

1. The flame will bend when linear fire source approaches to the curved sidewall, and a thicker smoke layer will be formed. Moreover, the maximum transverse temperature is at the vertical impact area above fire source.
2. For fire sources of same fuel, the heat release rate is mainly influenced by the heat feedback and area of fire source. When fire source approaches to the sidewall, heat release rate of fire source with aspect ratio lower than 42.5:1 increases due to the heat feedback is dominant. While heat release rate decreases of fire source with aspect ratio greater than or equal to 42.5:1 due to insufficient oxygen supply, and the influence of sidewall on air entrainment is dominant.
3. The effective ceiling height under curved ceiling is modified, the vertical distance between the fire source and plume impinge point and the arc length from impinge point to ceiling center is taken as the modified effective ceiling height. Therefore, a modified empirical formula to predict the longitudinal temperature distribution of linear fire sources with different sizes at different transverse positions is proposed. This formula is only applicable beyond the plume impinging area. Moreover, the ventilation coefficient is obtained, which can represents the correlation of temperature under different sealing situation.
4. Based on dimensionless analysis, it's concluded that the maximum ceiling temperature mainly influenced by heat release rate. What's more, it is validated that ventilation coefficient can predict the maximum ceiling temperature rise under sealing. Besides, an

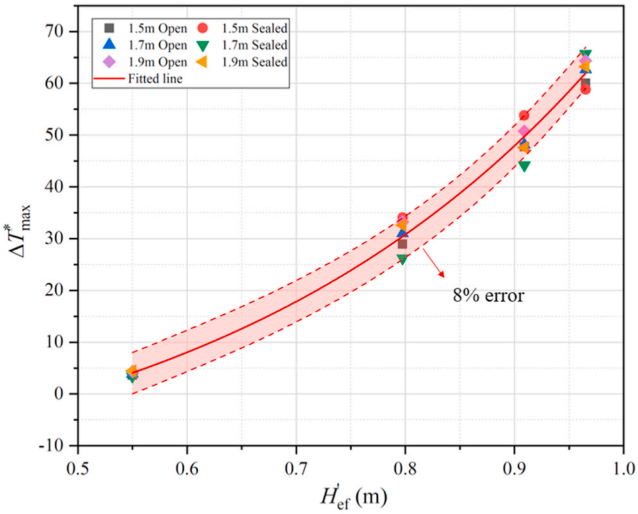

(a) Correlation diagram of modified effective ceiling height and dimensionless maximum temperature rise

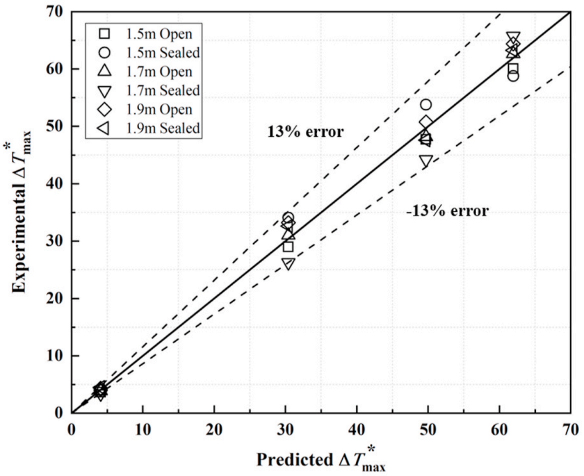

(b) Regression analysis of dimensionless maximum temperature rise

Fig. 7. The predicted formula and regression analysis of dimensionless maximum temperature rise.
(a) Correlation diagram of modified effective ceiling height and dimensionless maximum temperature rise
(b) Regression analysis of dimensionless maximum temperature rise

empirical formula to predict the maximum ceiling temperature rise is proposed, and the error between predicted value and experimental value is within 13%.

CRediT authorship contribution statement

Gang Xu: Conceptualization, Data curation, Investigation, Methodology, Writing – original draft, Writing-revised draft. **Guoqing Zhu:** Funding acquisition, Project administration, Resources, Supervision, Writing – review & editing. **Rongliang Pan:** Conceptualization, Data curation, Investigation, Methodology, Writing – original draft. **Xin Liu:** Formal analysis, Software, Validation.

Declaration of competing interest

The authors declare that they have no known competing financial interests or personal relationships that could have appeared to influence the work reported in this paper.

Acknowledgements

The work was supported by the National Key Research and Development Program of China (No.2016YFC0802900).

References

[1] P.F. Wang, G.Q. Zhu, R.L. Pan, T.W. Chu, Z. Wang, H.N. Liu, Effects of curved sidewall on maximum temperature and longitudinal temperature distribution induced by linear fire source in utility tunnel, Case Studies Thermal Eng. 17 (2020), 100555.

[2] F. Tang, L.J. Li, W.K. Chen, C.F. Tao, Z. Zhan, Studies on ceiling maximum thermal smoke temperature and longitudinal decay in a tunnel fire with different transverse gas burner locations, Appl. Therm. Eng. 110 (2017) 1674–1681.

[3] T.N. Zhou, Q.P. Chen, X.H. Wang, J.F. Zhao, C. Ding, J. Wang, The burning rate of n-heptane pool fires with constraint effect beneath an curved ceiling, Fuel 233 (2018) 825–833.

[4] Z.H. Liang, G.Q. Zhu, H.N. Liu, X. Zhou, Flame characteristic and ceiling temperature distribution under the effect of curved sidewall, Case Studies Thermal Eng. 14 (2019).

[5] C. Wei, S. Long, Z.C. Shi, M. Peng, H. Yang, S.G. Zhang, X.D. Cheng, Effect of train fire location on maximum smoke temperature beneath the subway tunnel ceiling, Tunn. Undergr. Space Technol. 97 (2020).

[6] C.F. Du, M. L Bian, Numerical simulation of fluid solid coupling heat transfer in tunnel, Case Studies Thermal Eng. 12 (2018) 117–125.

[7] Y.J. Gao, G.Q. Zhu, S.N. Gu, H.J. Tao, Y.C. Zhao, Experimental and numerical studies on ceiling maximum smoke temperature and longitudinal decay in a horseshoe shaped tunnel fire, Case Studies Thermal Eng. 12 (2018) 134–142.

[8] L. Gong, L. Jiang, S.Y. Li, N. Shen, Y.C. Zhang, J.H. Sun, Theoretical and experimental study on longitudinal smoke temperature distribution in tunnel fires, Int. J. Therm. Sci. 102 (2016) 319–328.

[9] J. Jie, T.T. Tan, Z.H. Gao, H.X. Wan, Influence of sidewall and aspect ratio on burning behaviors of rectangular ethanol and heptane pool fires, Fuel 238 (2019) 166–172.

[10] C.G. Fan, J. Yang, M.H. Li, A theoretical and experimental study of flame length under a tunnel ceiling, J. Therm. Anal. Calorim. 128 (2) (2017) 1143–1149.

[11] X. Zhou, G.Q. Zhu, H.N. Liu, Z.H. Liang, Experimental investigation on the influence of linear fire source along the wall on the temperature distribution in tunnel, Case Studies Thermal Eng. 14 (2019).

[12] Y.Z. Yao, X.D. Cheng, S.G. Zhang, K. Zhu, H.P. Zhang, L. Shi, Maximum smoke temperature beneath the ceiling in an enclosed channel with different fire locations, Appl. Therm. Eng. 111 (2017) 30–38.

[13] C.K. Chen, Y.L. Zhang, P. Lei, W.B. Jiao, A study for predicting the maximum gas temperature beneath ceiling in sealing tactics against tunnel fire, Tunn. Undergr. Space Technol. (2020) 98.

[14] H.N. Liu, G.Q. Zhu, R.L. Pan, M.M. Yu, Z.H. Liang, Experimental investigation of fire temperature distribution and ceiling temperature prediction in closed utility tunnel, Case Studies Thermal Eng. 14 (2019).

[15] Y.Z. Li, B. Lei, H. Ingason, The maximum temperature of buoyancy-driven smoke flow beneath the ceiling in tunnel fires, Fire Saf. J. 46 (4) (2011) 204–210.

[16] B.S. Grove, J.G. Quintiere, Calculating entrainment and flame height in fire plumes of axisymmetric and infinite line geometries, J. Fire Protect. Eng. 12 (3) (2002) 117–137.

[17] T.N. Zhou, Y. Zhou, C.G. Fan, J. Wang, Experimental study on temperature distribution beneath an curved tunnel ceiling with various fire locations, Tunn. Undergr. Space Technol. 98 (2020).

[18] R.L. Pan, G.Q. Zhu, P.F. Wang, X. Zhou, Z.H. Liang, H.N. Liu, G. Xu, Experimental investigation of maximum temperature and longitudinal temperature distribution induced by linear fire in portals-sealed tunnel, Case Studies Thermal Eng. 23 (2021).

[19] Y. Oka, H. Oka, O. Imazeki, Ceiling-jet thickness and vertical distribution along flat ceilinged horizontal tunnel with natural ventilation, Tunn. Undergr. Space Technol. 53 (2016) 68–77.

[20] Y. Utiskul, J.G. Quintiere, An application of mass loss rate model with fuel response effects in fully-developed compartment fires, Fire Saf. Sci. 9 (2008) 827–838.

[21] V. Babrauskas, Estimating large pool fire burning rates, Fire Technol. 19 (4) (1983) 251–261.

[22] R.L. Pan, G.Q. Zhu, Z.H. Liang, G.W. Zhang, H.N. Liu, X. Zhou, Experimental study on the fire shape and maximum temperature beneath ceiling centerline in utility tunnel under the effect of curved sidewall, Tunn. Undergr. Space Technol. 99 (2020).

[23] J. Ji, T.T. Tian, Z.H. Gao, H.X. Wan, Influence of sidewall and aspect ratio on burning behaviors of rectangular ethanol and heptane pool fires, Fuel 238 (2019) 166–172.

[24] H. Ingason, Z.L. Ying, A. Lonnermark, Tunnel Fire Dynamics, Springer, New York, 2015.

[25] Z.H. Gao, J. Ji, H.X. Wan, J.P. Zhu, J.H. Sun, Experimental investigation on transverse ceiling flame length and temperature distribution of sidewall confined tunnel fire, Fire Saf. J. 91 (2017) 371–379.

[26] X.C. Zhang, L.H. Hu, W. Zhu, X.L. Zhang, Z.Y. Li, Flame extension length and temperature profile in thermal impinging flow of buoyant round jet upon a horizontal plate, Appl. Therm. Eng. 73 (1) (2014) 15–22.

[27] Y.Z. Li, H. Ingason, The maximum ceiling gas temperature in a large tunnel fire, Fire Saf. J. 48 (2011) 38–48.

[28] H. Kurioka, Y. Oka, H. Satoh, et al., Fire properties in near field of square fire source with longitudinal ventilation in tunnels, Fire Saf. J. 38 (4) (2003) 319–340.

[29] Y.Z. Yao, K. He, M. Peng, L. Shi, X.D. Cheng, H.P. Zhang, Maximum gas temperature rise beneath the ceiling in a portals-sealed tunnel fire, Tunn. Undergr. Space Technol. 80 (2018) 10–15.